

Numerical Investigation on Performance of Coal Gasifier of 150kW under Various Injection Conditions

Hyeongyeong Choi^{a*}, Jaeseung Suh^a, Taihyeop Lho^b

^aSentech Co., Room 303, Inno Biz Park, Hannam Univ., 1646 Yuseong-daero, Yuseong-gu, Daejeon, Korea

^bNational Fusion Research Institute, 169-148 Gwahak-ro, Yuseong-gu, Daejeon, Korea

*Corresponding author: chk89418@esentech.kr

1. Introduction

Integrated coal gasification combined cycle (IGCC) has gained a lot of interest because they can produce cleaner gaseous fuels such as hydrogen, carbon monoxide and methane. This study focuses on the 150kW gasifier which is used in the National Fusion Research Institute (NFRI) plant. It is a fusion plasma technology to existing coal gasifier for better efficiency of low-carbon fuels. The cold gas is generated by reacting oxidants to coal with plasma technology of high temperature. The purpose of this study is to get the highest cold gas efficiency varied according to oxidant/coal injection amount, location and feeding gas. It is considerably complicated and expensive that cold gas efficiency is experimentally compared for all cases. Therefore, it is important to determine optimum operating condition using a computational fluid dynamics (CFD) model. It is possible to predict flow patterns, tracks of particles, combustion characteristics, temperature distributions and chemical distributions using the commercial CFD solver ANSYS/FLUENT.

2. Methods and Results

2.1 Numerical methods

Figure 1 shows characteristics for analysis of the 150kWe gasifier. The three-dimensional flows in gasifier includes in the turbulence, dispersion, mixing, chemical physical reaction of gas, devolatilization of the coal particles, volatile matter and char partial combustion etc. In addition, the heat transfer occurs by convection and radiation. So this steady stated CFD analysis is performed with gas-phase and char reaction models, turbulence models, discrete phase models (DPM) and thermal radiation models. Table I shows numerical model used in FLUENT code [1].

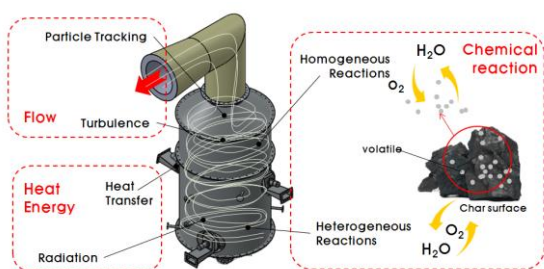


Fig.1. View of 150kW gasifier and general characteristics

Table I: Numerical models used in FLUENT

Analysis system	- Three-dimensional, steady stated flows - Mass, velocity (x, y, z), temperature, thermal radiation, and turbulence equation
Physical model	- Turbulence: Realizable k-ε model - Particle: DPM (with random walk model) - Radiation: P1 thermal radiation model
Chemical model	- Char gasification: Multiple surface reaction model - Finite-rate/eddy-dissipation model

The physical gasification of coal is evaporation and devolatilization by heating coal. Namely, the coal particle is divided into the char, volatiles and moistures.



Then, homogeneous reactions of volatiles and heterogeneous reactions of char take place. The kinetic rate expressions for global reactions for both heterogeneous and homogeneous reactions are given by relationship as [2, 3, 4]:

$$k = AT^{\beta} e^{-Ea/RT} \quad (2)$$

The char gasification reactions take place after volatiles in the coal particles are released. The heterogeneous reactions are modeled by multiple surface reaction mechanism [5]. The chemical reactions in the gas-solid interaction include reaction of char particle with oxygen, steam and carbon dioxide and the major products of surface reactions are hydrogen and carbon monoxide [6]. The reactions considered in this model along with reaction rate information are summarized in table II. The char gasification reactions are given as [2]:

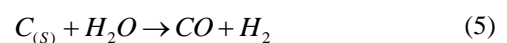


Table II : Kinetic rate parameters for char reaction

Char reaction	A	Ea (J/kmol)	β
1	5.67E+09	1.60E+08	0
2	1.60E+12	2.24E+07	0
3	8.55E+04	1.40E+08	0

The gas phase reactions take place in the reduction reaction and gasification zone of the entrained flow gasifier. The turbulence chemistry interaction is modeled using a finite rate/eddy dissipation model, a built in module in FLUENT [5, 7]. The homogeneous reactions of volatiles considered in this model along with kinetic parameters are summarized in Table III [1].

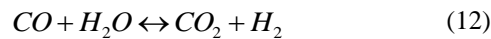
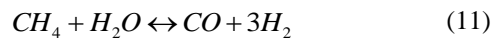
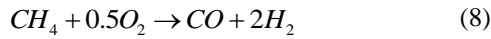
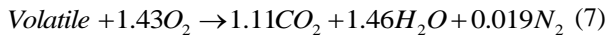
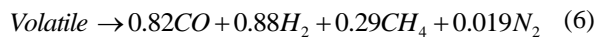


Table III : Kinetic rate parameters for gas phase reaction

Gas reaction	A	Ea (J/kmol)	B
6	1.60E+15	1.00E+08	0
7	2.13E+12	2.03E+08	0
8	3.00E+08	1.26E+08	-1
9	6.80E+15	1.68E+08	0
10	2.20E+12	1.67E+08	0
11 (forward)	4.40E+11	1.68E+08	0
11 (reverse)	5.12E-14	2.73E+04	0
12 (forward)	2.75E+10	8.38E+07	0
12 (reverse)	2.65E-02	3.96E+03	0
12 (reverse)	26.5	6.58E+08	0

2.2 Geometry and mesh

Fig.2 shows the internal flow field of 150kw gasifier. Coal is transported with the feeding gas through the torch, and oxidant is injected through tangential ports. Torch is two at the top of reactor, and one at the bottom of reactor. Torch supplies not only coal but also steam and heat. There are two tangential ports on the top and bottom of reactor, respectively. In addition, some air is supplied through the two view port. Exhaust duct is modeled as an extended structure.

The grids are shown in Fig. 3. The total number of cells is approximately 1 million in the internal flow field. The shape of the cells is tetrahedrons as body fitted grids. These have inflated boundary on the walls of gasifier. The number of inflated layers is 4. Each torch and ports has finer grids.

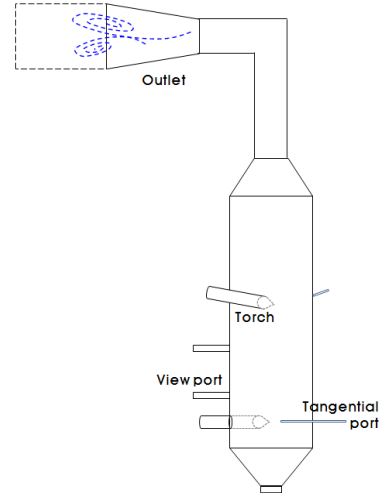


Fig.2. Views of the internal flow field for CFD modeling

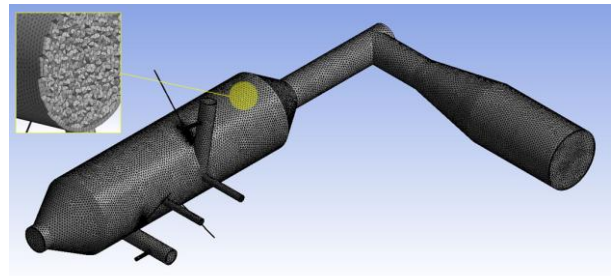


Fig.3. Views of the internal flow field for CFD modeling

2.3. Operating conditions

Table IV show proximate analysis, ultimate analysis and measurement result of the calorific value for Indonesia lower coal burnt used in NFRI. A diameter (D_{coal}) of the coal particles is less than $70 \mu\text{m}$ in their experiments, and is assumed to have a uniform particle size of $50 \mu\text{m}$ for this analysis. Then the coal combustion and char gasification reaction are assumed to take place only in surface of the coal particles.

Oxidant is oxygen and steam, and feeding gas is air or carbon dioxide. Table V shows inlet conditions varied according to injection amount of oxidant and coal and feeding gas. Feeding gas is carbon dioxide in case 2, and air in the others. The injection amount of oxidant and coal in case 3 and 4 is more than case 1 and 2. The injection power is the same in all cases. The heat loss is assumed 100kW/m^2 in the wall of reactor, and 400kW/m^2 in the exhaust duct, either

Table IV: Design coal of NFRI coal gasifier

Proximate analysis of design coal			
Moisture (%)	33.99	Fixed carbon (%)	28.78
Volatile (%)	33.10	Ash (%)	4.13
Ultimate analysis of design coal			
C (%)	67.33	H (%)	5.04
O (%)	22.50	N (%)	0.91
S (%)	0.09	Ash (%)	4.13
Input HHV		4190.0 Kcal/kg	

Table V: Design coal of NFRI coal gasifier

Case 1						
		steam	coal	oxygen	air	power
		kg/hr		lpm		kW
Torch	top	26	30		100	40
	bottom	14	30		100	30
Torch Barrier	top				50	
	bottom				50	
Tangential Port	top	20				
	bottom			330		
Viewport	top				50	
	bottom				50	
Case 2 – Feeding gas: Carbon dioxide						
		steam	coal	oxygen	carbon dioxide	power
		kg/hr		lpm		kW
Torch	top	26	30		100	40
	bottom	14	30		100	30
Torch Barrier	top				50	
	bottom				50	
Tangential Port	top	20				
	bottom			330		
Viewport	top				50	
	bottom				50	
Case 3						
		steam	coal	oxygen	air	power
		kg/hr		lpm		kW
Torch	top	26	80		100	40
	bottom	14	40		100	30
Torch Barrier	top				50	
	bottom				50	
Tangential Port	top	30				
	bottom			500		
Viewport	top				50	
	bottom				50	
Case 4						
Torch	top	26	80		100	40
	bottom	14	40		100	30
Torch Barrier	top				50	
	bottom				50	
Tangential Port	top	20		150		
	bottom	10		350		
Viewport	top				50	
	bottom				50	

2.4 Results

Figs. 4~7 show contours of static temperature for each case. For all cases, the highest temperature is performed by the combustion reaction of coal and oxygen at bottom of the reactor. The temperature is gradually reduced to go to the upper. However, temperature rises slightly at the top of the reactor for case 4 because oxygen is injected at the top of the reactor. The average temperature of exit of gasifier is more than 1400 K.

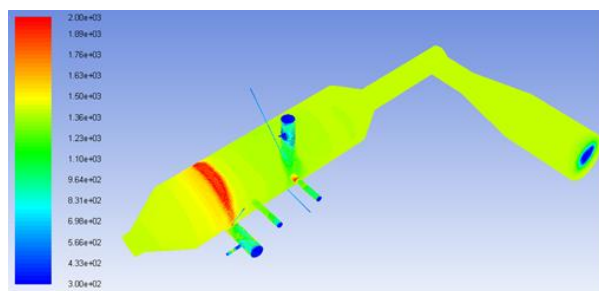


Fig.4. Contours of static temperature of case 1

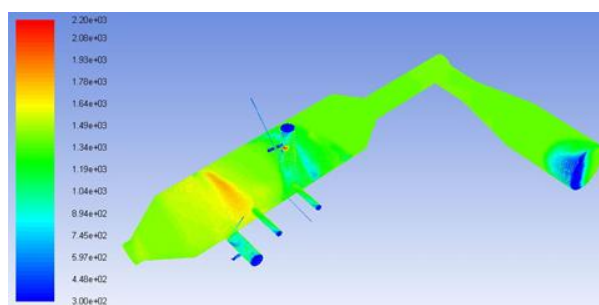


Fig.5. Contours of static temperature of case 2

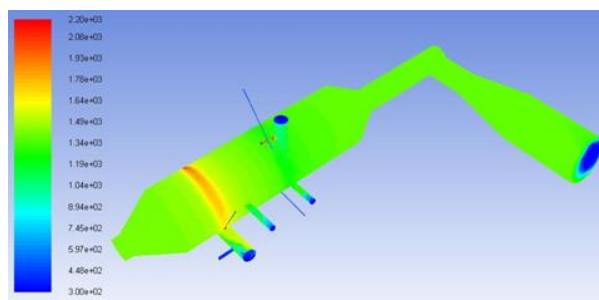


Fig.6. Contours of static temperature of case 3

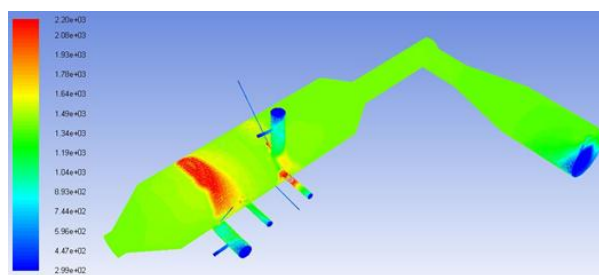


Fig.7. Contours of static temperature of case 4

Contours of mole fraction of steam are shown in figs. 8 and 9. Steam is injected through 2 tangential ports at top of reactor and three torches. Then, it is immediately removed by chemical reaction in fig.8 for case 1. Most of the cases are similar. However, in fig.9 for case 2, the chemical reaction is hardly generated than other cases. The chemical reaction of equation 4 is actively made due to the large amount of carbon dioxide. The chemical reaction of eq. 5 is relatively reduced in char gasification. So there remain excess steams in the gasifier. Or it is assumed that excess steams increase in the reverse reaction of eq. 5.

Figs. 10~13 show contours of mole fraction of carbon dioxide. Most of carbon dioxide is generated by chemical reaction of eq. 10. This reaction is exothermic in which carbon monoxide is oxidized to carbon dioxide. The temperature is too high when the carbon dioxide occurs as shown in figs. 4 and 10. A high mole fraction of carbon dioxide is shown in fig. 11 because feeding gas is carbon dioxide in case 2. A low mole fraction of carbon dioxide is shown in fig. 12 for case 3. Oxygen and steam were already exhausted from the char reaction because the amount of coal has doubled, and not involved in gas phase reactions which generate carbon dioxide. Conversely the lowest mole fraction of carbon monoxide is shown in fig.15 for case 2, and the highest mole fraction of carbon monoxide is shown in fig.16 for case 3.

Figs. 18~21 show contours of mole fraction of hydrogen. The hydrogen is generated by the reduction reaction of steam. The mole fraction of hydrogen is constant from generated to exhaust duct. For case 2, most of hydrogen is generated by char reaction of eq. 5. Fig. 19 shows that hydrogen is generated from top of reactor which steam is fed to.

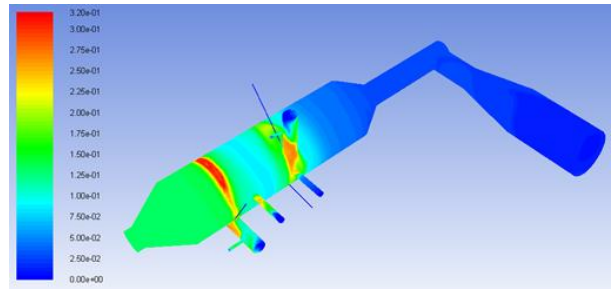


Fig.10. Contours of mole fraction of CO₂ of case 1

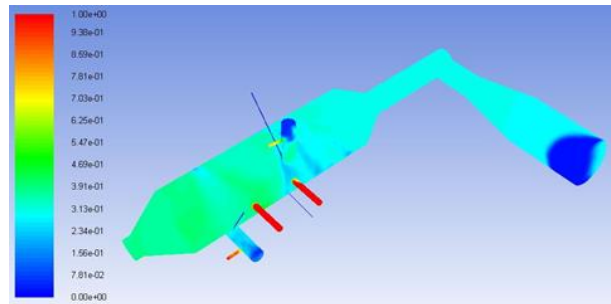


Fig.11. Contours of mole fraction of CO₂ of case 2

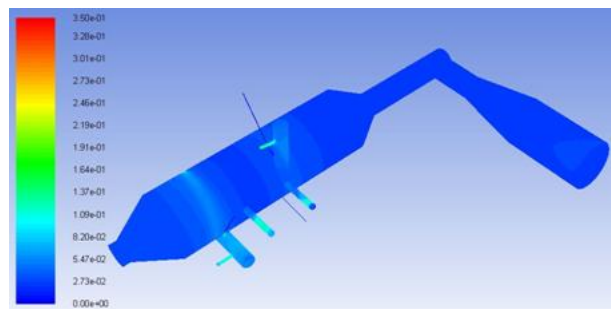


Fig.12. Contours of mole fraction of CO₂ of case 3

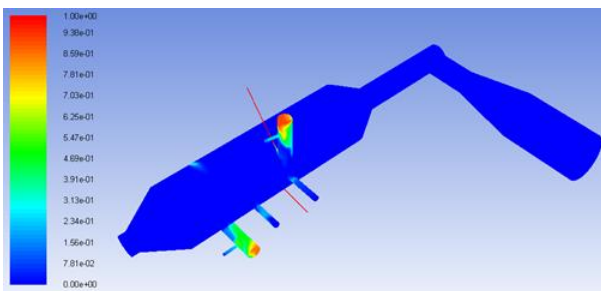


Fig.8. Contours of mole fraction of H₂O of case 1

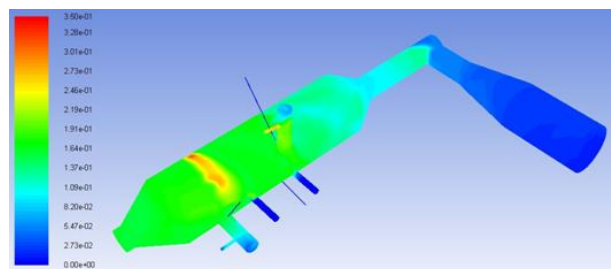


Fig.13. Contours of mole fraction of CO₂ of case 4

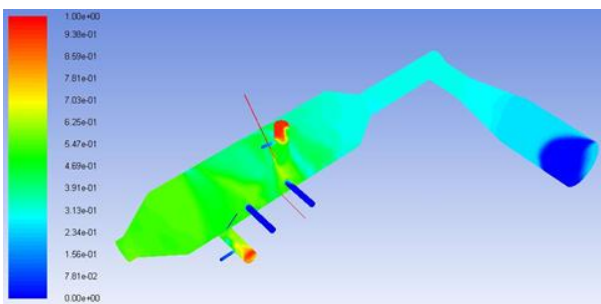


Fig.9. Contours of mole fraction of H₂O of case 2

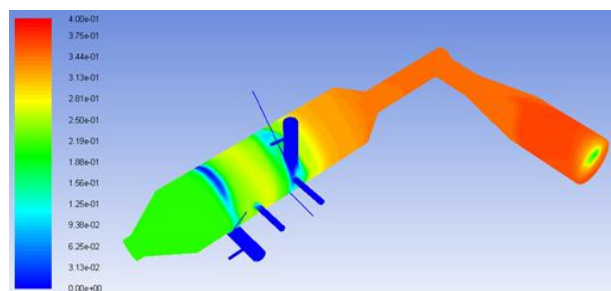


Fig.14. Contours of mole fraction of CO of case 1

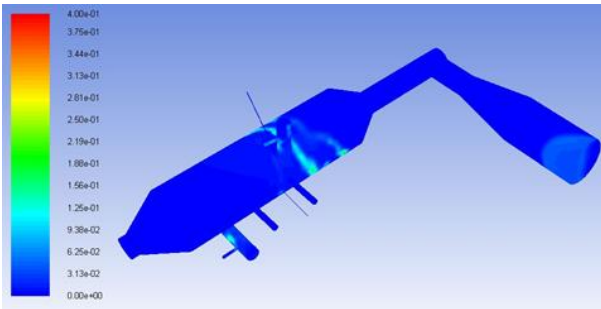


Fig.15. Contours of mole fraction of CO of case 2

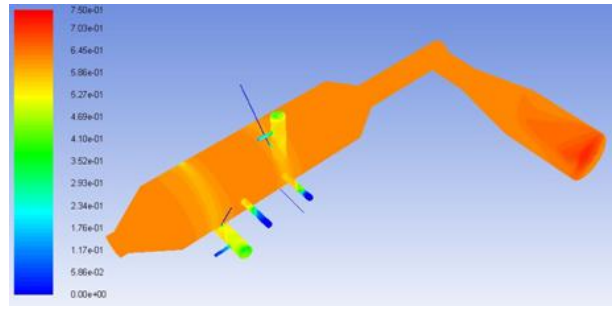


Fig.20. Contours of mole fraction of H2 of case 3

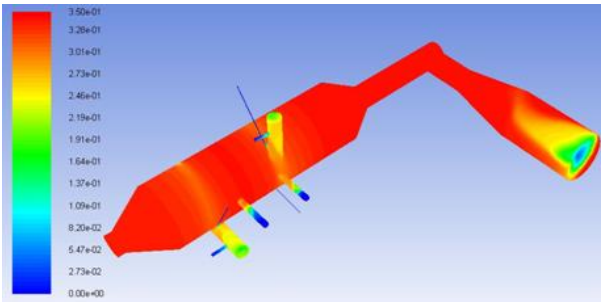


Fig.16. Contours of mole fraction of CO of case 3

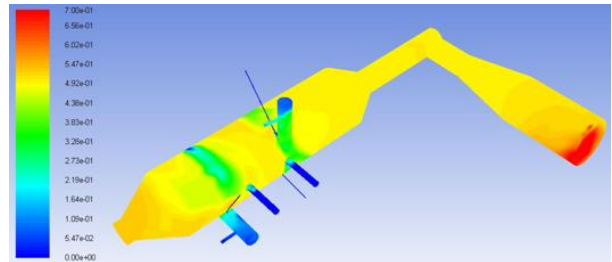


Fig.21. Contours of mole fraction of H2 of case 4

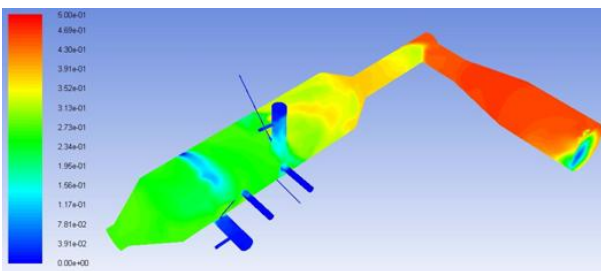


Fig.17. Contours of mole fraction of CO of case 4

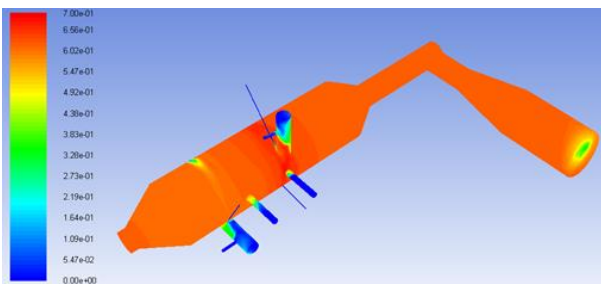


Fig.18. Contours of mole fraction of H2 of case 1

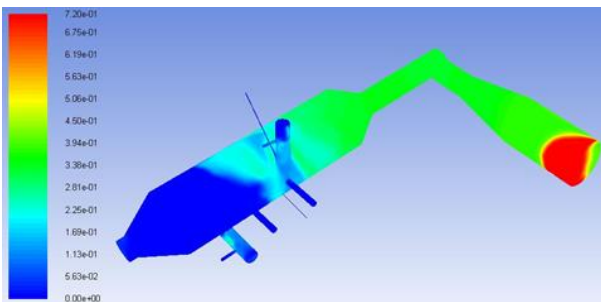


Fig.19. Contours of mole fraction of H2 of case 2

3. Conclusions

This study has numerical investigation for the phenomena of coal gasification for coal gasifier of 150kW at various operating conditions. The results are summarized in table VI. The cold gas efficiency is best in case 1, and worst in case 2. The air as feeding gas is more efficient than carbon dioxide, and the amount of coal that is important to find the appropriate value for the capacity of the gasifier than strictly greater.

Table VI: Results of analysis with mole fraction at exit

Case	Mole fraction (%)			Carbon exchange rate (%)	Cold gas efficiency (%)
	H2	CO	CO2		
1	58.21	32.37	5.15	82.51	161.24
2	37.92	0	29.4	63.73	60.73
3	62.78	33.96	2.29	79.48	143.07
4	50.05	43.68	4.46	85.79	113.25

REFERENCES

- [1] C. Lee, B. Jung, J. Lee and Y. Yun, Modeling and Simulation on the Reacting Flow Field and the Performance of Coal Gasifier by Using CFD Method, International Journal of Advanced Mechanical Engineering, vol. 4, no. 1, pp. 15~20
- [2] J. Hong, S. Park, J. Song, J. Hwang, Numerical Study on 300 MW Shell-Type One-Stage Entrained Flow Bed Gasifier : Effect of Coal·Biomass Blending Ratio on CO₂ Gasification, Trans. of the Korean Hydrogen and New Energy Society, vol. 23, no. 3, pp. 274~284

- [3] E. Biagini et al., Devolatilization rate of biomass and coal-biomass blends: an experimental investigation, vol. 81
- [4] H. Watanabe, and M. Otaka, Numerical simulation of coal gasification in entrained flow coal gasifier, vol. 85
- [5] ANSYS workbench FLUENT manual, 2010
- [6] B.W. Brown, L.D. Smoot, P.J. Smith and, P.O. Hedman, Measurement and Prediction of Entrained-Flow Gasification Processes, AIChE Journal, vol. 34, pp.435~446
- [7] P. P. Mashingo, G. R. John, C. F. Mhilo, Performance Prediction of a Pressurized Entrained Flow Ultra-Fine Coal Gasifier, Modeling and Numerical Simulation of Material Science, 4, 70-77